Environ Geol (2008) 56:729–740
DOI 10.1007/s00254-008-1332-y

SPECIAL ISSUE

Laboratory simulation showing the influence of salt efflorescence on the weathering of composite building materials

G. Cultrone · E. Sebastián

Received: 4 March 2008 / Accepted: 7 April 2008 / Published online: 19 April 2008

Abstract A common decay scenario in old and new buildings was simulated: the effects on masonry structures of salt efflorescence or subefflorescence produced by the rise of saline solution. Eight different types of masonry wall each made up of a combination of different construction materials (brick, calcarenite and four types of mortar were combined as follows: pure lime mortar, mortar + air entraining agent, mortar + pozzolana, mortar + air entraining agent + pozzolana) have been tested. These materials have different textures (strong anisotropy in brick, irregular-shaped pores in calcarenite, retraction fissures or rounded pores in mortars which also show a reduction of porosity along the contact area with the stone), different hydric behaviours (under total immersion brick + mortar specimens absorb water faster than calcarenite + mortar specimens) and different pore size distribution (brick shows unimodal pore distribution, whereas calcarenite and mortars are bimodal). In the salt weathering test, mortars interlayered with masonry blocks did not act as sacrificial layers. In fact, they allowed salts to rise through them and crystallize on the brick or calcarenite pieces causing the masonry structure to decay. Only the addition of an air-entraining agent partially hindered the capillary rise of the salt-laden solutions.

Keywords Masonry walls · Efflorescence and subefflorescence · Porosity · Weathering

G. Cultrone (✉) · E. Sebastián
Department of Mineralogy and Petrology,
University of Granada,
Avda. Fuentenueva s/n,
18002 Granada, Spain
e-mail: cultrone@ugr.es

Introduction

Architectural heritage is subjected to a range of decay processes which endanger its future conservation in many of the world's historic city centres. Salt crystallization is one of the most common causes of such decay (Charola 2000; Espinosa et al. 2008; Lubelli et al. 2006a, b; Price 1996; Winkler 1987). Salts generally come from air pollution, ground water rising up through foundations and sea-spray deposition, or through the use of inappropriate treatments or incompatible building materials (Cardell et al. 2003; Moreno et al. 2006).

The location of salt crystallization depends on the flow of the water and the permeability of the substrate, which allows the salt to move. The crystallization of salt crystals is accompanied by an increase in volume, which produces internal stresses (Benavente et al. 2007; Evans 1970). While the liquid phase allows salt to be transported, evaporation, which can occur outside (efflorescence) or inside the material (subefflorescence), enables it to crystallize. It is not unusual for both forms of florescence to occur together. The magnitude of the pressure depends partly on the kind of salt involved and partly on the size and shape of the capillary pore system (Benavente et al. 2007; Grossi and Esbert 1994; Ruiz Agudo 2007; Van et al. 2007; Winkler 1987). When the crystallization pressure exceeds the tensile strength of the material, the material cracks (Espinosa et al. 2008; La Iglesia et al. 1997). Furthermore, the longer the saline solution remains within the porous media, the worse the damage may be (Benavente et al. 2003, 2004).

The feasibility of removing salts from stone materials has been widely investigated (Ciabach and Skibinski 1989; Lubelli and Van Hess 2007; Maravelaki Kaalitzaki 2007; Watt and Colston 2000), and it has been demonstrated that

salts can be dangerous even if protective or consolidating products are used (Van Hess and Brocken 2004). In terms of masonry structures, a construction material is just one part of a more complex structure, in the sense that each block is joined to its neighbours by a mortar (Binda et al. 1997 and 2000; Larbi 2004; Van Hess and Brocken 2004). Hall and Hoff (2002) have described how water moves through composite materials, whether layered or formed by random particle inclusions (i.e. particles with different properties dispersed within the matrix of a porous material). It has been observed that the selective decay of composite materials when subjected to salt attack may be due to the fact that they have different compositions, porous systems and hydraulic conductivity (Cooper et al. 1989; Gonçalves et al. 2007; Kuchitsu et al. 1999; Petkovic et al. 2007; Poli et al. 2007). Schiavon et al. (1995) detected that Ca-rich lime mortars and limestones can play an important role in the sulphate weathering of building stones. Moreover, the degradation of masonry is particularly intense within the near-surface region of the two joined materials, where the retention of solution allows salt to crystallize and lets the decay progress inwards (Haneef et al. 1992). In some cases, the use of unsuitable materials during restoration work worsened the damage caused to the masonry by salt crystallization (Veniale et al. 2003; Lubelli et al. 2006a, b). It is important to underline that this problem occurs frequently in both old and new buildings.

Aim of this work is to study the decay of masonry walls due to the efflorescence (or subefflorescence) of salt solution produced by capillary rise (a common decay scenario in many buildings). This study seeks to determine how salts act on masonries, and how the damage is distributed amongst the different components of a masonry structure (i.e. whether or not the mortar acts as a sacrificial buffer against the forces of decay).

Simulated weathering tests on brick + mortar and calcarenite + mortar masonry specimens specially designed and assembled in the laboratory were carried out. Brick, calcarenite and mortar are very common construction materials and have different porous systems and hydric behaviours (Cultrone et al. 2004, 2008; Lawrence et al. 2007).

Materials

Lime-based mortars were chosen because they are compatible with traditional construction materials (Cultrone et al. 2004; Groot et al. 1999; Moropoulou et al. 2005). Four types of lime mortar were prepared using siliceous sand as the aggregate (the abbreviation for each group of mortars is shown in brackets): pure lime (L), lime + air-entraining agent (LA), lime + pozzolana (LP), lime + pozzolana + air-entraining agent (LPA). The binder/aggregate ratio per volume was 1:3. The weight percentage of the additives was 0.1 vol.% for the air-entraining agent (according to the recommendations of the manufacturer) and 20 vol.% for the pozzolana, a volcanic ash, as recommended in the UNE 80-301-87 standard for cements (1987). Further details on the mineralogy and the texture of these mortars can be found in Cultrone et al. (2005).

Bricks (B) were prepared using a Plio-Pleistocenic clay from the Guadix Formation (Granada, Spain) which was rich in quartz and phyllosilicates and contained lesser amounts of feldspars. Bricks were fired in an electric oven (Herotec CR-35) at 950°C. After firing, the only significant mineralogical change was the formation of mullite at the expense of illite/muscovite (Cultrone et al. 2001).

The other construction material was a Tortonian biocalcarenite (a packstone according to the Dunham classification, 1962) (C) from the Calcarenitic Unit (Santa Pudia Quarry, Granada, Spain) which was used in the building of a large number of Granada's most emblematic monuments (Cathedral, Royal Chapel, La Cartuja, Carlos V Palace in the Alhambra). It contains a great variety of bioclasts cemented together by sparitic carbonate (Luque et al. 2008).

Composite materials were made up of a mortar sandwiched between two pieces of brick or calcarenite. The brick and calcarenite blocks measured $5 \times 4 \times 3$ cm^3 (long × wide × high), and the mortar measured $5 \times 4 \times 1$ cm^3 making the total dimensions of each masonry specimen $5 \times 4 \times 7$ cm^3.

Bricks or calcarenites were combined with four types of mortars, resulting in eight different masonry specimens: B + L, B + LA, B + LP, B + LPA, C + L, C + LA, C + LP and C + LPA. The specimens were put into a CO_2-saturated climatic chamber (Kesternick) for 30 days to accelerate the carbonation process in the mortars.

Methods

Analysis of the mineralogy and texture of masonry specimens was performed with a polarized optical microscope Olympus BX-60.

The parameters associated with fluid uptake and transport inside the pores were determined by hydric tests. Since the decay processes often depend on the transport of water inside porous solids (Charola 2004), these tests were important for determining the durability of these materials. Water absorption (UNI-EN-13755 2002), drying (NORMAL 29/88 1988) and capillary uptake (UNI-EN-1925 2000) were determined by weighing the specimens (three samples per group) at regular intervals. The absorption

coefficient, the drying rate, the real and apparent density and the open porosity were calculated from the values thus obtained (UNI-EN-1936 2007).

Sodium sulphate is considered one of the most dangerous of the different salts detected in historical buildings, because of its strong crystallisation pressure when, by absorbing water, it hydrates from thenardite (anhydrous phase) to mirabilite (decahydrate phase) (Linares Fernández et al. 2002; Neville 2004). The damage caused by sodium sulphate is attributable to three mechanisms: crystallization, hydration and thermal expansion (Price 1996; Pye and Schiavon 1989). Rodríguez Navarro et al. (2000) demonstrated that the hydration of Na_2SO_4 is a two-step process: dissolution and re-precipitation. The molar volume of this salt may increase by up to 240 times when it changes from the anhydrous to the decahydrate phase (La Iglesia et al. 1997). Winkler and Singer (1972) calculated that mirabilite can exert a pressure of 473 atm in pores and fissures depending on the temperature and the supersaturation of the solution. Recently, Steiger (2005a, b) calculated the crystallization pressure for supersaturated solutions of different types of salt and observed that the growth pressure of a salt increases as pore entrance size decreases.

The Na_2SO_4 saturate solution was prepared in the laboratory under controlled environmental conditions (20°C and 50% relative humidity) and was decanted for 24 h to eliminate any undissolved sulphate crystal. A measure of 172.4 g salt in 1 litre of deionized water was added to saturate the solution. The saline solution was poured into cylindrical glass beakers (110 ml solution each beaker) and the masonry specimens were placed inside (Fig. 1). The saline solution was only in contact with the lower part of the specimens (i.e. brick or calcarenite). It was not in contact with either the mortar or the mortar-stone contact surface. The solution was covered with a layer of molten paraffin wax to avoid excessive evaporation and to promote the capillary rise of the solution through the pore system of the masonry specimens. The gradual increase in salt efflorescence and the resulting surface damage on the specimens were photographically recorded using time-lapse methods. The solution evaporation rate was measured by continuous weighing of the specimen + solution + wax + beaker system using Mettler PM600 scales which have an accuracy of 0.01 g.

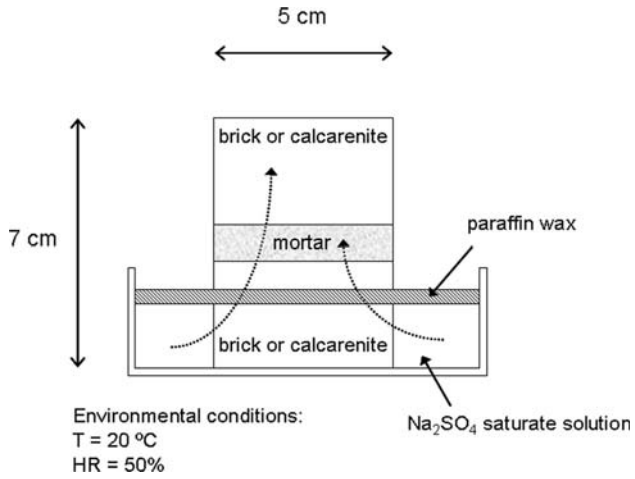

Fig. 1 Diagram showing the set up of the salt efflorescence test. Only the lower part of the brick or calcarenite is in contact with the saline solution. The dotted arrows indicate the ascent of the solution inside the masonry specimens which then crystallizes as efflorescence or subefflorescence

The mineralogy of the salts crystallized in the eight masonry specimens was investigated by X-ray diffraction (XRD) using a Philips PW-1710 diffractometer with graphite monocromator, automatic slit and Cu$K\alpha$ radiation, 3 to 60°2θ explored area and 0.01°2θ s^{-1} goniometer speed. The resulting data were interpreted using XPowder software (Martín 2004).

The change in porosity before and after crystallization was appraised using mercury intrusion porosimetry (MIP), and the textural appearance was analysed using field emission scanning electron microscopy (FESEM). The pore access size distribution was studied using a Micromeritics Autopore III 9410 porosimeter with a maximum injection pressure of 414 MPa. Damaged and undamaged specimen chips of ca. 2 cm^3 were analysed. To evaluate the binding or disintegrating effect of the Na_2SO_4 on the damaged composite materials, these specimens were not water cleaned so as not to remove the weathering products. Two MIP measurements were carried out per sample. Details of the texture of brick, calcarenite and mortars were studied using a Leo Gemini 1530 FESEM coupled with an Oxford INCA-200 microanalysis system. Secondary electron (SE) and back-scattered electron (BSE) images were collected using small sample pieces (5 × 5 × 3 mm^3 in size) or polished carbon-coated thin sections. The acceleration beam current was 25 kV.

Results and discussions

Optical microscopy

Brick and calcarenite

The temper used in the bricks, which is composed almost entirely of metamorphic quartz, has grains of up to 1.5 mm (Fig. 2a). The matrix is dark-reddish with low birefringence due to the partial vitrification of the bricks. Brick texture shows a strong anisotropy because of the orientation of the phyllosilicates that occurs during the moulding

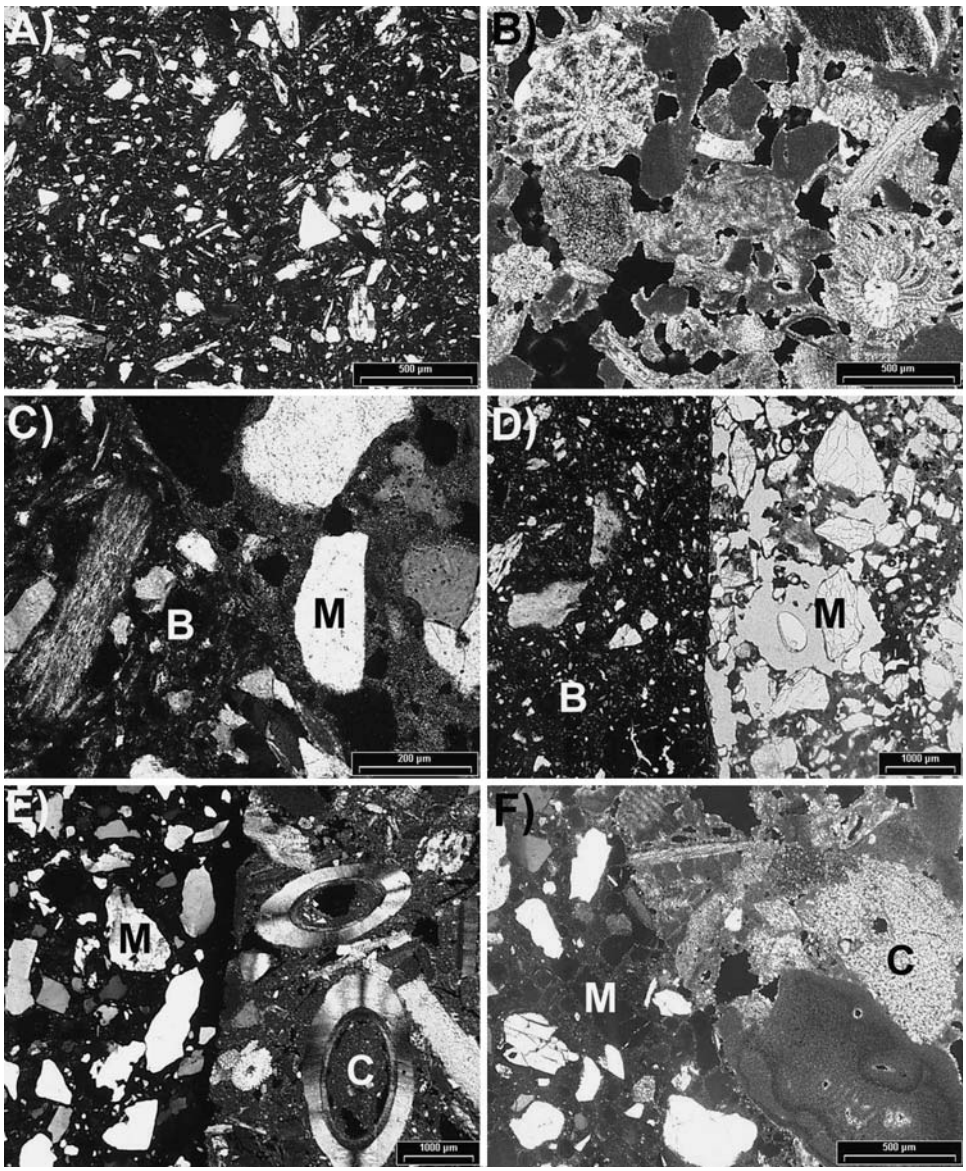

Fig. 2 **a–d** Optical microscopy results for brick (**a**), calcarenite (**b**) and masonry specimens (**c**, **d**, **e**, **f**). Quartz fragments and dehydroxylated phyllosilicates dispersed in a dark matrix are observed in bricks (**a**, **c**, **d**); a great variety of bioclasts and irregular shaped pores are shown in calcarenites (**b**, **e**, **f**); sub angular to round quartz grains constitute the aggregate of LA (**c**), LP (**d**), L (**e**) and LPA (**f**) mortar samples. In masonry specimens, brick, calcarenite and mortar materials are indicated as *B*, *C* and *M*, respectively

of clayey material. After firing at 950°C the phyllosilicates in the matrix can no longer be seen, only pseudomorphs after former crystals can be observed which are situated parallel to the largest face of the bricks (5×4 cm^2, the face in contact with the mortars). This feature and the partial vitrification of the bricks provide a slight adherence to the mortars. On the contrary, the rough surface texture of calcarenites enables them to bind better to the corresponding mortar block. They are composed of fragments of molluscs, echinoderms and foraminifers that are well cemented together by micritic and sparitic calcium carbonate (Fig. 2b). Occasionally quartz, muscovite, biotite and feldspar fragments can be seen dispersed in the matrix from metamorphic rock formations surrounding the Granada Basin. The pores in bricks are irregular or elliptical in shape (Fig. 2a). In calcarenite they are larger and also irregular in shape (Fig. 2b).

Mortars

Mortars seem to be well cemented together because the union between the micritic calcite (binder) and the grains of quartz (aggregate) is continuous and complete. The appearance of the mortars varies depending on the additive used. In the case of mortars without additive (L), some irregular-shaped pores and drying cracks can be seen (Fig. 2e). The air-entraining agent (LA) produces very round pores in the mortars, and there are no drying fissures (Fig. 2c). The presence of pozzolana causes the colour of the binder to change from white to grey. As in the two

Table 1 Hydric parameters of bricks (B) or calcarenites (C) plus lime (L), lime + air entraining agent (LA), lime + pozzolana (LP), lime + air-entraining agent + pozzolana (LPA)

	A_F	A_C	D_I	S	P	ρ_A	ρ_R	C	C_C
B + L	19.80	12.63	0.23	85.54	33.09	1.67	2.50	2.65	0.31
B + LA	20.57	12.42	0.23	84.91	33.76	1.65	2.49	1.77	0.34
B + LP	19.56	11.44	0.24	84.81	32.96	1.68	2.51	2.49	0.31
B + LPA	20.28	11.80	0.23	84.10	33.23	1.65	2.47	2.41	0.34
C + L	13.04	9.06	0.22	80.13	23.28	1.85	2.41	1.51	0.33
C + LA	13.89	7.89	0.23	80.94	24.53	1.80	2.39	1.12	0.18
C + LP	14.09	7.26	0.25	79.62	24.96	1.81	2.42	1.49	0.18
C + LPA	12.97	9.00	0.22	78.97	22.92	1.84	2.38	1.35	0.23

A_F = free absorption; A_C = absorption coefficient; D_I = drying index; S = saturation coefficient; P = open porosity; ρ_A = apparent density; ρ_R = real density; C = capillarity; C_C = capillarity coefficient

previous mortar groups, the pores in LP are angular (Fig. 2d) whereas in LPA they are rounded (Fig. 2f).

Hydric tests

Brick + mortar masonry specimens always show higher water absorption figures under total immersion (A_F, Table 1) and higher absorption coefficients (A_C) than calcarenite + mortar specimens (Fig. 3a, b). It is evident that it is the brick and the calcarenite and not the mortars (these represent ~14% of the total volume of the masonry) that affect the capacity of these masonry specimens to absorb water. All bricks + mortar specimens show a higher real density (ρ_R) than calcarenites + mortar, whereas the latter have a higher apparent density (ρ_A). This suggests that calcarenites have more empty spaces. Moreover, the values for open porosity (P) and for saturation (S) are higher in bricks + mortar specimens, suggesting the presence of more interconnected pore spaces and/or fissures in the latter. Specimens with a hydraulic mortar and without an air-entraining agent (B + LP and C + LP) take longer to dry, a fact confirmed by their higher desorption rates (D_I is 0.24 and 0.25, respectively). The use of an air-entraining agent causes air bubbles to be produced in the mortars and this reduces the density of the masonry specimens. The water absorption by capillarity is higher in brick + mortar specimens (Fig. 3c, d; C, Table 1). When the air-entraining agent is added to mortars (LA and LPA) the presence of air bubbles causes a decrease in capillary absorption. The addition of the air-entraining agent therefore has the effect of creating closed porosity. Results for the capillary test showed smaller differences between the respective behaviour of the two masonry groups than those for the test for water absorption by total immersion. The results of the latter test show that the 14% mortar-volume masonry specimens have a considerable influence on water absorption by capillarity. On this question, Hendry (2002) observed that, even if mortars generally represent only a small part of the total volume of a masonry structure they can have a disproportionately large influence on its performance.

FESEM observations

FESEM microphotographs show the sheet-like fabric of the phyllosilicates in bricks (Fig. 4a). These minerals display a

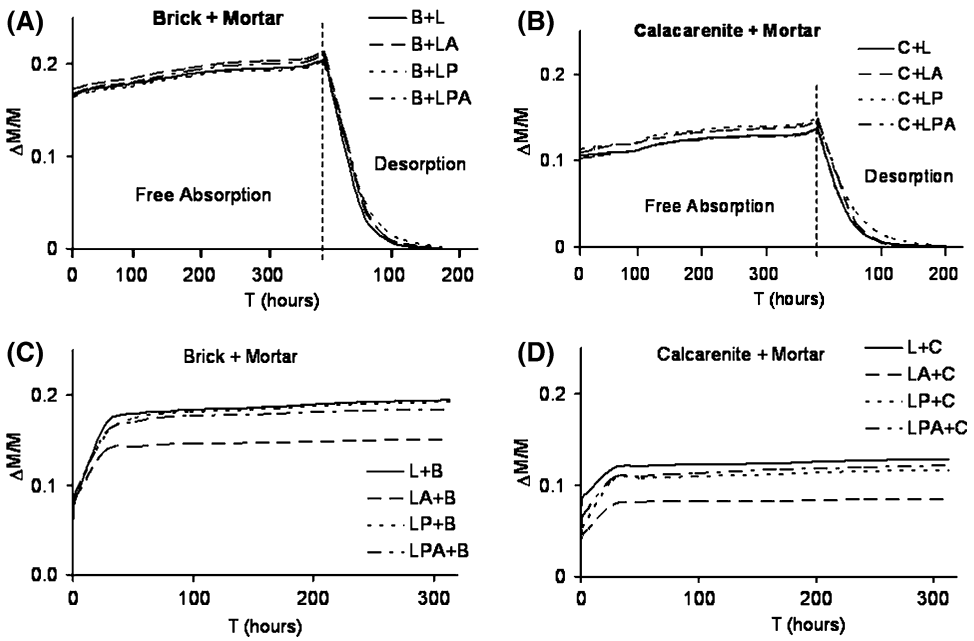

Fig. 3 **a–d** Free water absorption, desorption (**a**, **b**) and capillary curves (**c**, **d**) for brick + mortar and calcarenite + mortar masonry specimens over time (in hours)

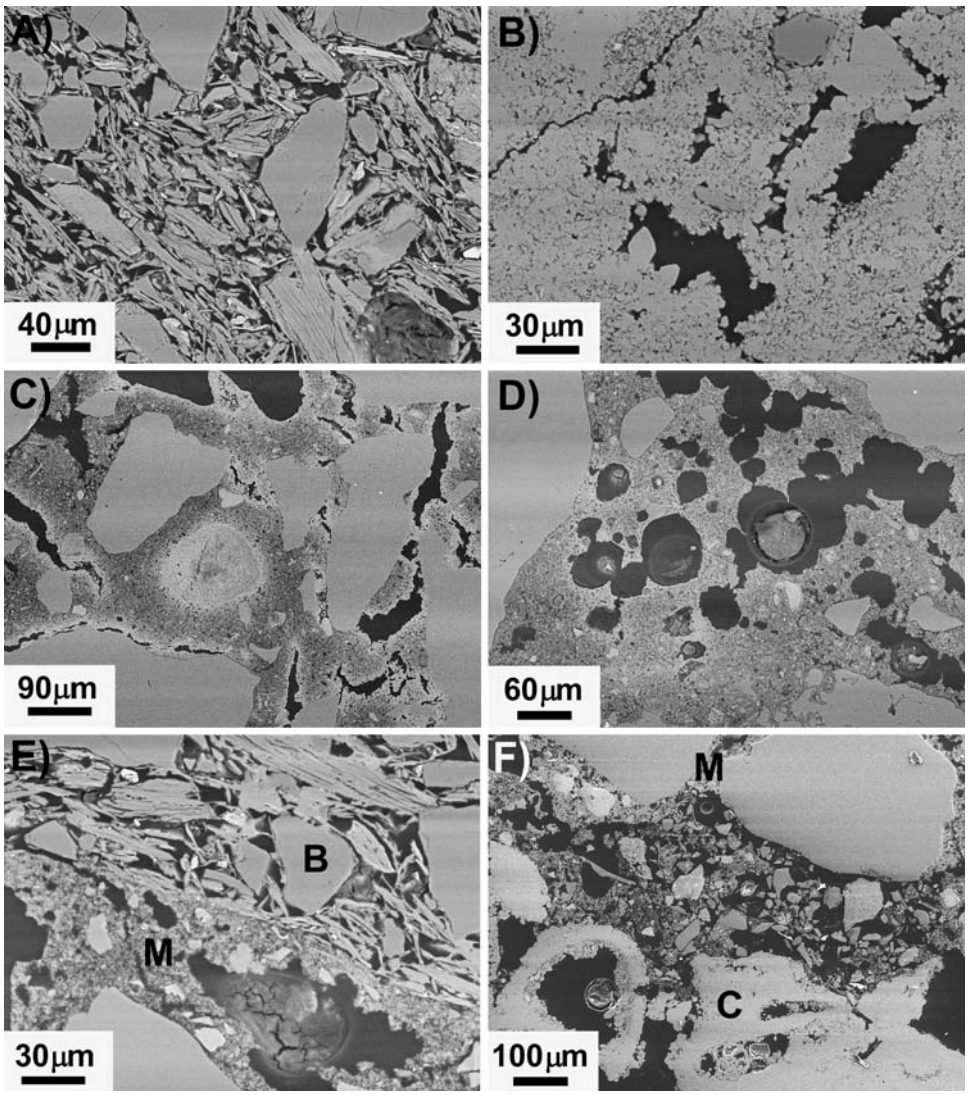

Fig. 4 **a–f** FESEM microphotographs show the orientation of dehydroxylated phyllosilicates and quartz grains in brick (**a**); the growth of scalenohedric calcite crystals in irregular pores in calcarenite (**b**); drying cracks in pure lime mortar (**c**); the development of rounded pores in lime mortar + air entraining agent (**d**); B + LP (**e**) and C + LPA (**f**) contact area. In **e** and **f**, brick, calcarenite and mortar materials are indicated as *B*, *C* and *M*, respectively

marked exfoliation along their basal planes due to the loss of K^+ and OH^- groups during firing (Rodríguez Navarro et al. 2003). Quartz grains are irregular in both size and shape.

The bioclasts in calcarenites are cemented together by sparitic calcite (Fig. 4b). Large and irregular pores can be observed inside which scalenohedric calcite crystals usually grow.

The main difference between the mortars is the appearance of drying cracks in pure lime mortars (L, Fig. 4c) and in the specimens with added pozzolana (LP). The addition of an air-entraining agent, however, favours the development of air bubbles and reduces the drying cracks in LA and LPA mortars (Fig. 4d).

A reduction in the porosity of the mortars along the contact surface with brick or calcarenite is noticed. This is because the binder tends to concentrate in this thin layer (Fig. 4e, f). In fact, during the preparation of the masonry specimens, the mortars had still not set when they were joined to the bricks or calcarenites, and the adhesive forces between water molecules and the brick or calcarenite surface favoured the propagation of a calcium-rich solution in this area.

Salt crystallization test

The evaporation rate of the saline solution is similar in brick + mortar and calcarenite + mortar specimens (Fig. 5a, b) and slightly higher when pozzolana is added to mortars (LP and LPA). The results indicate that a small volume of mortar influences the intensity of salt induced decay. The composite materials reach a constant weight after 20 days testing. Analysing the four brick + mortar masonry specimens, it is interesting to notice how saline solution evaporation varies depending on the different combinations of additives in the mortars. B + LA and B + LPA specimens behave very differently (Fig. 5a). Both mortars are prepared with an air entraining agent. But

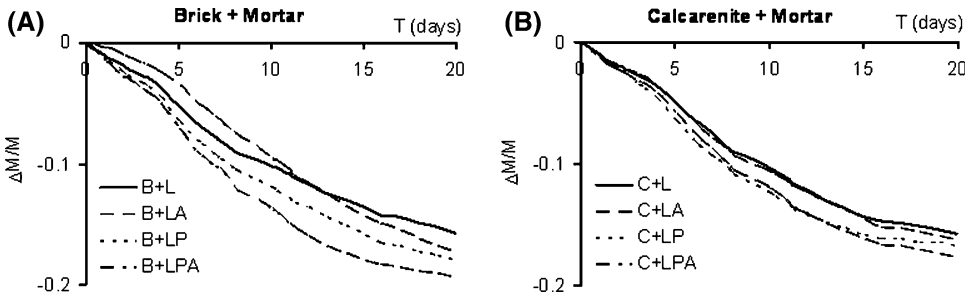

Fig. 5 **a–b** Weight loss (due to the evaporation of the saline solution through the porous stone) of brick + mortar (**a**) and calcarenite + mortar (**b**) masonry specimens over time

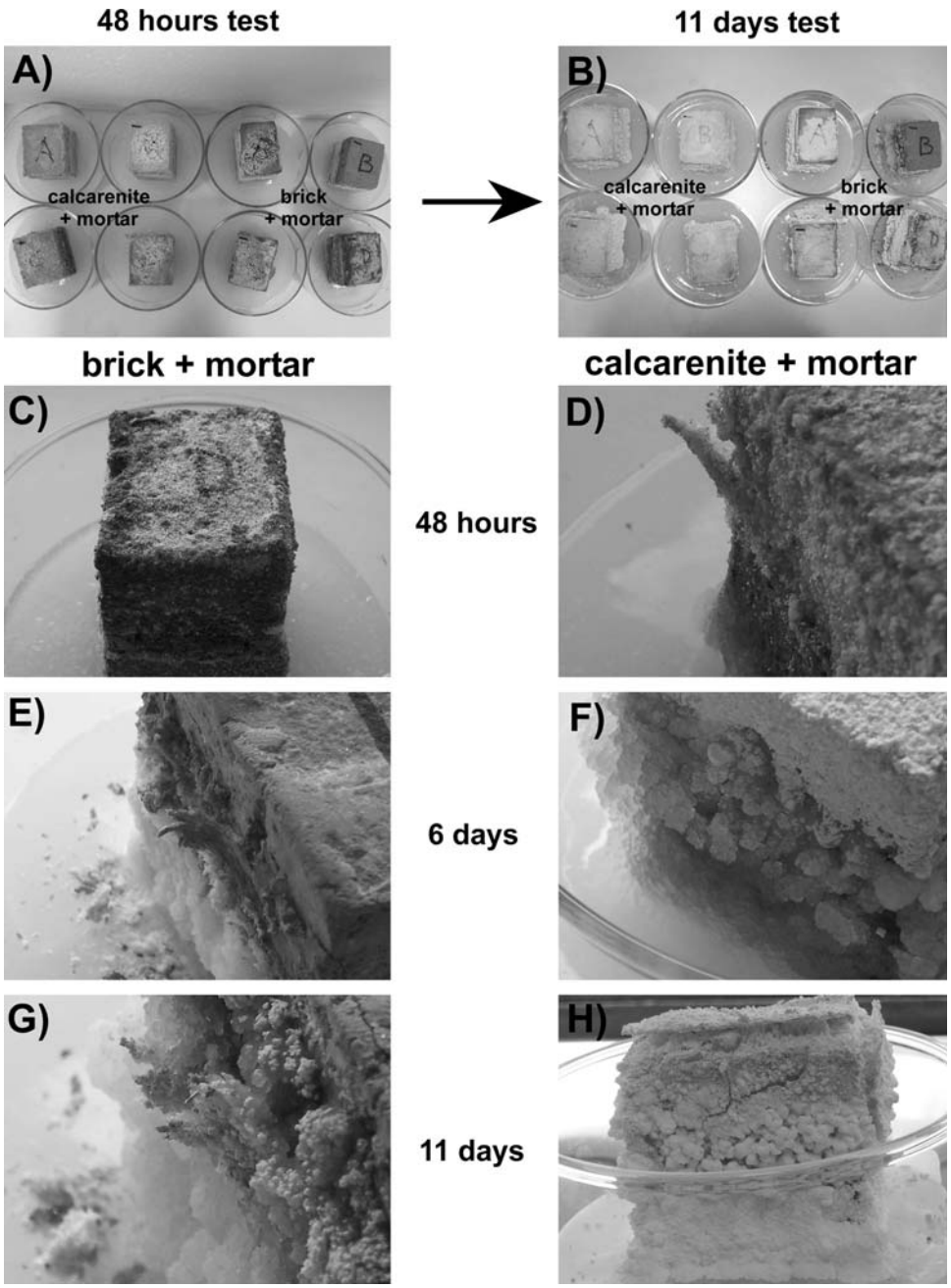

Fig. 6 **a–h** Time-lapse photographs of masonry specimens after 48 h, 6 and 11 days of salt saturated solution flow-through and evaporation-crystallisation. **a** and **b** illustrate a general view of efflorescence growth during the test; **c**, **e** and **g** show details of brick + mortar specimens, and **d**, **f** and **h** are calcarenite + mortar specimens

while in B + LA the flux of the solution inside the mortar is greatly hindered by the air bubbles which reduce the interconnectivity between the pores inside the mortar, in B + LPA the connection between the pores seems to be facilitated by the volcanic ash particles (20% of total) which help the solution to move through the mortar. This

result is confirmed by the higher capillarity (C) of the B + LPA sample compared with B + LA (Table 1). As the evaporation of the solution progresses, more changes are registered: B + LP and B + LPA curves tend to diverge, whereas the B + L and the B + LA curves converge after 11 days. In calcarenite + mortar masonry systems the differences between the specimens are smaller (Fig. 5b). They follow two parallel lines: one showing the curves for C + L and C + LA in which the solution evaporates slowly, and the other showing C + LP and C + LPA in which it evaporates faster. These results confirm the important role that the addition of pozzolana may have in accelerating the rise of salt laden solution through masonry walls.

In terms of sample deterioration, mortars did not act as sacrificial layers in masonry structures. After just 24 h, saline solution had migrated through mortars and crystallized on brick or calcarenite pieces as efflorescence and subefflorescence depending on the evaporation speed of the solution at the stone surface and the resulting movement of the crystallization boundary (Rodríguez Navarro et al. 2002). Figure 6a, b shows the 8 different masonry specimens after 48 h and 11 days of the decay test. At the end of the test, only the upper part of B + LA and part of C + LA were free of salts, which indicate that in these combinations it was difficult for the salt solution to rise. The specimens suffered loss of small fragments in the early stages of this test (Fig. 6c, d), a phenomenon that occurred especially in samples in which pozzolana was added to the mortars. After 6 days sodium sulphate continued to crystallize inside and outside the masonry specimens causing flaking in B + LA (Fig. 6e) or causing 2–3 mm-thick granular crusts to develop in C + LP (Fig. 6f). After 11 days, large salt crystals had developed on the brick surface causing cracks (Fig. 6g), whereas in calcarenite + mortar specimens large thin flakes of calcarenite had broken off pushed out by acicular salt crystals (Fig. 6h). This difference suggests that surface evaporation in calcarenite is higher than that in brick specimens. In C + LA and B + LA specimens, in which the air-entraining agent was added to mortars, deterioration was less accentuated. The only changes detected in subsequent days were the progressive decay of the masonry specimens, especially those in which calcarenite was used.

Mineralogical analysis of the salts collected from the masonries revealed that there are no differences between the efflorescences that appeared on the bricks, mortars and calcarenites. They are composed almost completely of thenardite (Fig. 7a) and sometimes mirabilite is present (Fig. 7b). Rare calcite and quartz phases from the brick and calcarenite blocks were also detected. No other sulphates were identified.

Changes in masonry texture after simulated weathering test

The components of the masonries have different pore size distributions (Fig. 8). This condition can lead to damage in masonry structures especially along the contact surface between two different materials (Mendes and Philippi 2005). Before deterioration, the pore size distribution of brick peaks at around 1 μm, and it is the only material with unimodal distribution (continuous line, Fig. 8a). This pore range is responsible for the fast rate of water absorption detected in the hydric tests (Table 1; Fig. 3). Calcarenite and the four types of mortar are bimodal (continuous lines,

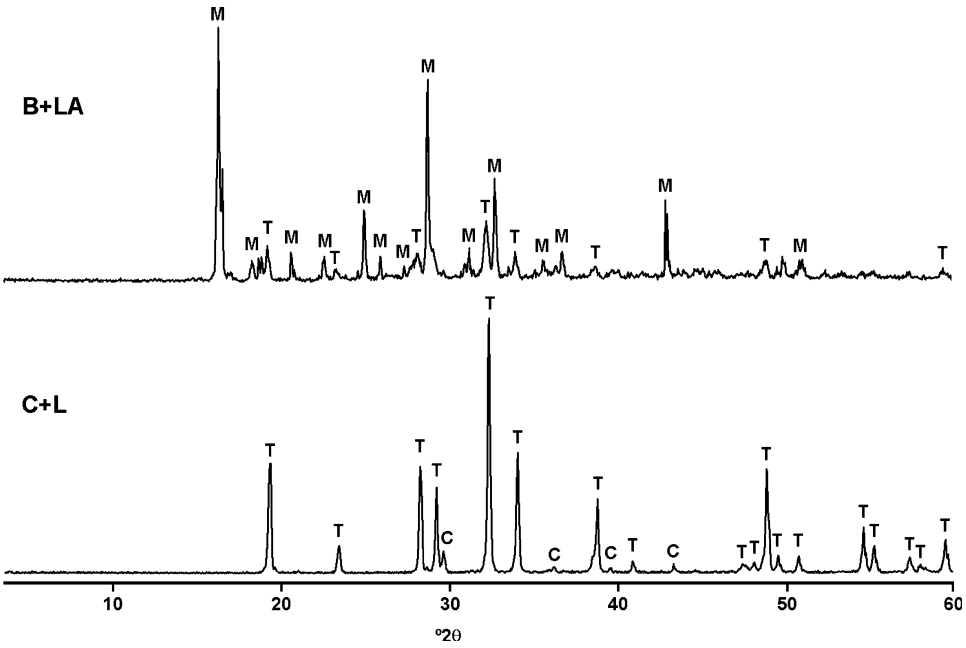

Fig. 7 **a–b** X-ray diffraction patterns of B + LA and C + L masonry specimens. Legend: *T* thenardite, *M* mirabilite, *C* calcite

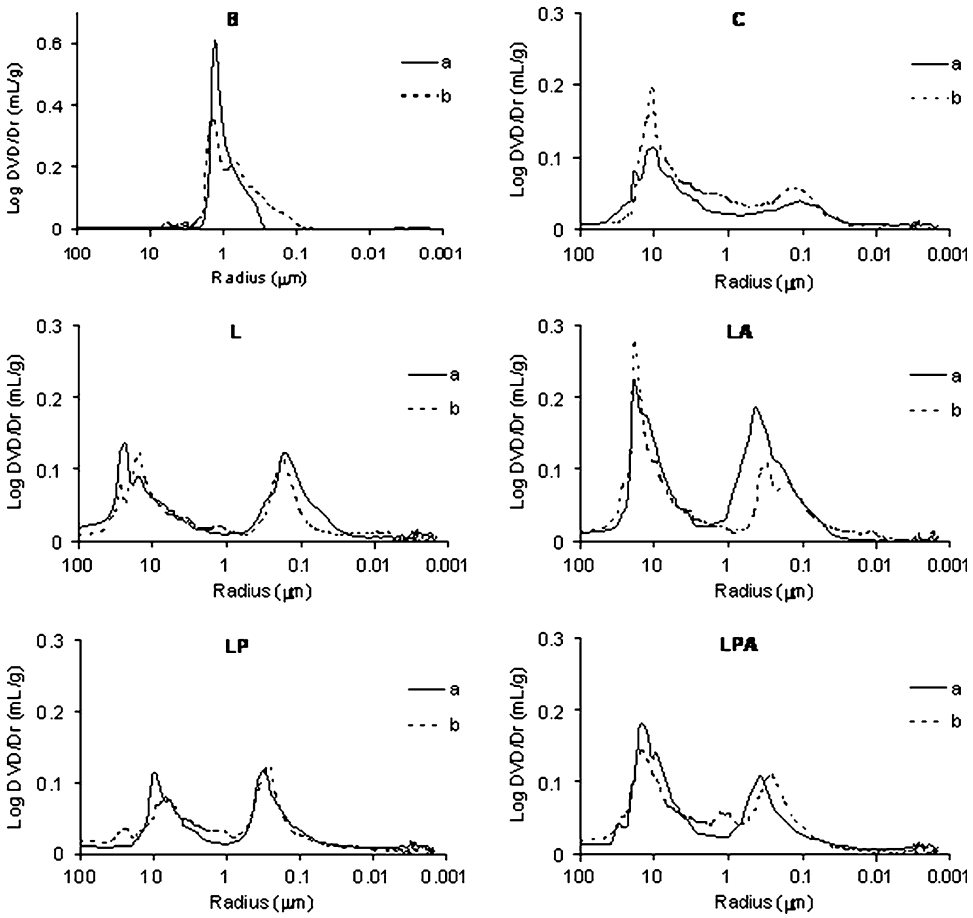

Fig. 8 **a–f** MIP pore size distribution curves of brick (*B*), calcarenite (*C*) and mortar specimens (*L*, *LA*, *LP* and *LPA*) before (*a*, continuous line) and after (*b*, dotted line) the salt efflorescence test

Fig. 8b–f). Calcarenite shows two families of pores with radii of approximately 10 and 0.1 μm, respectively. Those with the bigger radius are more common. In the case of lime mortars without additives (L) or with pozzolana (LP), the height of the two peaks on the graph is similar, with L mortars showing a greater distance between the values, whereas the presence of an air-entraining agent (mortars LA and LPA) means there are more large pores (10 μm) than small pores. After the salt efflorescence test a small volume of pores are filled with salts (dotted line, Fig. 8a–f). The general trend is for a shift of the curves towards smaller pores. This means that a new family of small pores (or microfissures) has been developed by crystallization pressure. The crystallization pressure is higher in this type of pore (Benavente et al. 2007; Scherer 1999) and is responsible for the decay of the structure.

FESEM observations demonstrate that salts concentrate indistinctly in mortars and in the upper brick or calcarenite units. The four types of lime mortar do not retain the saline solution in their body and instead allow it to migrate to the brick and calcarenite pieces (Fig. 6). Thenardite aggregates formed after dehydration of pre-existing mirabilite crystals

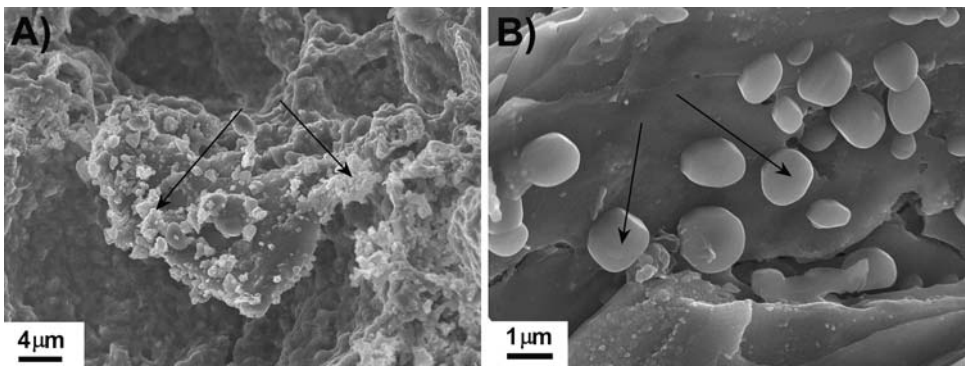

Fig. 9 **a–b** FESEM microphotographs of masonry specimens in which thenardite crystals can be seen. They generally appear as masses of micron-sized crystals that have replaced the mirabilite crystals (*black arrow*, **a**), but in some cases they precipitate directly from the solution as isolated crystals (*black arrow*, **b**)

are very common (Fig. 9a), although in some cases, thenardite crystals that had precipitated directly from the solution were also detected (Fig. 9b). This phenomenon is less usual, but a fast evaporation and a high degree of supersaturation solution in the micropores can induce the direct precipitation of thenardite which causes greater damage to porous materials than mirabilite does (Rodríguez Navarro and Dohene 1999; Rodríguez Navarro et al. 2000).

Conclusion

From the experimental results outlined earlier, the following conclusions can be drawn:

- The components of the masonries are mineralogically and texturally different: bricks are partially vitrified and show a marked anisotropy; calcarenites have rough surfaces and large pores; mortars are characterized by retraction fissures or rounded pores depending on the additive used. In addition, bricks are silicate-based materials, whereas calcarenites are calcareous and lime mortars are made up of silicates plus carbonates.
- A reduction in the porosity of the mortars was observed in the mortar—stone contact zone, because the binder tends to concentrate in this area.
- In this research, mortars are sandwiched between two pieces of brick or calcarenite and represent 14% of the total volume of the masonry specimens. Mortars seem to have no influence at all on the water absorption (by total immersion) behaviour of the building materials examined in this study. Bricks permit higher and faster water absorption than calcarenites because of their different pore size distribution. Interconnection between pores seems to be worse in calcarenites.
- The small volume of mortar (14%) influences water and saline solution absorption by capillarity. The mortars do not act as sacrificial layers in masonry specimens because they permit the migration and crystallization of Na_2SO_4 in brick and calcarenite pieces as efflorescence or subefflorescence.
- The damage observed in masonry specimens is similar to that observed on many buildings: cracking and loss of fragments. Salts fill a small volume of pores and cause the development of microcracks, which are responsible for masonry decay.
- The addition of an air entraining agent to lime mortars reduces the rise of saline solution, water and/or other fluids through the masonry because it creates closed porosity, thereby reducing damage to the structure.

This type of research provides new information on the durability of different combinations of building materials which vary greatly from a mineralogical and a textural point of view. It needs to be promoted to better understand the movement and crystallization of salts inside and outside masonry structures as this has fundamental implications for the conservation of cultural heritage and for civil engineering in general.

Acknowledgments This research has been supported by a Marie Curie Fellowship of the European Community Programme "Energy, Environment and Sustainable Development" under contract number EVK4-CT-2002-50006, the Research Group RNM179 of the Junta de Andalucía and the Research Project DGI MAT2000-06804. We thank the Centro de Instrumentación Científica of the Universidad de Granada for technical assistance during FESEM analyses and Nigel Walkington for the translation of the manuscript.

References

Benavente D, García del Cura MA, Ordóñez S (2003) Salt influence on evaporation from porous building rocks. Construct Build Mater 17:113–122

Benavente D, García del Cura MA, Fort R, Ordóñez S (2004) Durability estimation of porous building stones from pore structure and strength. Eng Geol 74:113–127

Benavente D, Martínez Martínez J, Cueto N, García del Cura MA (2007) Salt weathering in dual-porosity building dolostones. Eng Geol 94:215–226

Binda L, Modena C, Baronio G, Abbaneo S (1997) Repair and investigation techniques for stone masonry walls. Construct Build Mater 11:133–142

Binda L, Saisi A, Tiraboschi C (2000) Investigation procedures for the diagnosis of historic masonries. Construct Build Mater 14:199–233

Cardell C, Delalieux F, Roumpopoulos K, Moropoulou A, Auger F, Van Griegen R (2003) Salt-induced decay in calcareous stone monuments and buildings in a marine environment in SW France. Construct Build Mater 17:165–179

Charola AE (2004) Deterioration in historic buildings and monuments. Paper presented at the 10th International Congress on deterioration and conservation of stone, Stockholm (Sweden), vol 1, 3–14

Charola AE (2000) Salts in the deterioration of porous materials: an overview. J Am Inst Conserv 39:327–343

Ciabach J, Skibinski S (1989) Analyses of the total salt content and control of salt removal from stone historical objects. Paper presented at the 1° Simposio Internazionale "La conservazione dei monumenti nel bacino del Mediterraneo", Bari (Italy), pp 325–328

Cooper TP, Dowding P, Lewis JO, Mulvin L, O'Brien P, Olley J, O'Daly G (1989) Contribution of calcium from limestone and mortar to the decay of granite walling. Paper presented at the European Symposium "Science, Technology and European Cultural Heritage, Bologna (Italy), pp 456–461

Cultrone G, Rodríguez Navarro C, Sebastián E, Cazalla O, de la Torre MJ (2001) Carbonate and silicate phase reactions during ceramic firing. Eur J Mineral 13:621–634

Cultrone G, Sebastián E, Elert K, de la Torre MJ, Cazalla O, Rodríguez Navarro C (2004) Influence of mineralogy and firing temperature on porosity of bricks. J Eur Ceram Soc 24:547–564

Cultrone G, Sebastián E, Ortega Huertas M (2005) Forced and natural carbonation of lime-based mortars with and without additives: mineralogical and textural changes. Cem Concr Res 35:2278–2289

Cultrone G, Russo LG, Calabrò C, Urosevic M, Pezzino A (2008) Influence of pore system characteristics on limestone vulnerability: a laboratory study. Environ Geol (in press)
Dunham RJ (1962) Classification of carbonate rocks according to depositional texture. In: Classification of carbonate rocks. American Association of Petroleum Geologists Memoir (USA), pp 108–121
Espinosa RM, Franke L, Deckelmann G (2008) Model for the mechanical stress due to the salt crystallization in porous materials. Constr Build Mater (in press)
Evans IS (1970) Salt crystallization and rock weathering: a review. Revue de Geomorphologie dynamique 19:153–177
Gonçalves TD, Pel L, Delgado Rodrigues J (2007) Drying of salt-contamined masonry: MRI laboratory monitoring. Environ Geol 52:293–302
Groot C, Bartos P, Huges J (1999) Historic mortars: characteristics and test concluding summary and state of the art. In: International Workshop on Historic Mortars. Paisley (UK), pp 443–454
Grossi CM, Esbert RM (1994) Las sales solubles en el deterioro de rocas monumentales. Revisión Bibliográfica. Materiales de Construcción 44:15–29
Hall C, Hoff WD (2002) Water transport in brick, stone and concrete. Spon Press, London, New York
Haneef SJ, Dickinson C, Johnson JB, Thompson GE, Wood GC (1992) Simulation of the degradation of coupled stones by artificial acid rain. Stud Conserv 37:105–112
Hendry EA (2002) Masonry walls: materials and construction. Constr Build Mater 15:323–330
Kuchitsu N, Ishizaki T, Nishiura T (1999) Salt weathering of brick monuments in Ayutthaya, Thailand. Eng Geol 55:91–99
La Iglesia A, González V, López Acevedo V, Viedma C (1997) Salt crystallization in porous construction materials. I. Estimation of crystallization pressure. J Cryst Growth 177:111–118
Larbi JA (2004) Microscopy applied to the diagnosis of the deterioration of brick masonry. Constr Build Mater 18:299–307
Lawrence RM, Mays TJ, Rugby SP, Walter P, D'Ayala D (2007) Effects of carbonation on the pore structure of non-hydraulic lime mortars. Cem Concr Res 37:1059–1069
Linares Fernández L, Rodríguez Navarro C, Sebastián Pardo E, de la Torre López MJ, Cultrone G, Cazalla O (2002) Efecto de aditivos en la cristalización de sulfato sódico. Boletín de la Sociedad Española de Mineralogía 25A:49–50
Lubelli B, Van Hess RPJ (2007) Effectiveness of crystallization inhibitors in preventing salt damage in building materials. J Cult Herit 8:223–234
Lubelli B, Van Hees RPJ, Groot GWP (2006a) Investigation on the behaviour of a restoration plaster applied on heavy salt loaded masonry. Constr Build Mater 20:691–699
Lubelli B, Van Hees RPJ, Groot GWP (2006b) Sodium chloride crystallization in a "salt transporting" restoration plaster. Cem Concr Res 36:1467–1474
Luque A, Cultrone G, Sebastián E, Cazalla O (2008) Evaluation of the effectiveness of treatment products in improving the durability of a bioclastic limestone (Granada, Spain). Materiales de Construcción (in press)
Maravelaki Kaalitzaki P (2007) Hydraulic lime mortars with siloxane for waterproofing historic masonry. Cem Concr Res 37:283–290
Martín JD (2004) Using XPowder: a software package for powder X-ray diffraction analysis. http://www.xpowder.com. Legal Deposit GR 1001/04, Spain
Mendes N, Philippi PC (2005) A method for predicting heat and moisture transfer through multilayered walls based on temperature and moisture content gradients. Int J Heat Mass Transf 48:37–51
Moreno F, Vilela SAG, Antunes ASG, Alves CAS (2006) Capillary rising salt pollution and granitic stone erosive decay in the parish church of Torre del Moncorvo (NE Portugal). Implications for conservation strategy. J Cult Herit 7:56–66
Moropoulou A, Bakolas A, Moundoulas P, Aggelakopoulou E, Anagnostopoulou S (2005) Strength development and lime reaction in mortars for repairing historic masonries. Cem Concr Res 27:289–294
Neville A (2004) The confused world of sulphate attach on concrete. Cem Concr Res 34:1275–1296
NORMAL 29/88 (1988) Misura dell'indice di asciugamento (drying index). CNR-ICR, Roma (Italy)
Petkovic J, Huinink HP, Pel L, Kopinga K, Van Hess RPJ (2007) Salt transport in plaster/substrate layers. Mater Struct 40:475–490
Poli T, Toniolo L, Valentini M, Bizzaro G, Melzi R, Tedoldi F, Cannazza G (2007) A portable NMR device for the evaluation of water presence in building materials. J Cult Herit 8:134–140
Price CA (1996) Stone conservation. An overview of current research. The Getty Conservation Institute, Santa Monica (USA)
Pye K, Schiavon N (1989) Cause of sulphate attack on concrete, render and stone indicated by sulphur isotope ratios. Nature 342:663–664
Rodríguez Navarro C, Cultrone G, Sánchez Navas A, Sebastián E (2003) Dynamics of high-T muscovite to mullite transformation: a TEM study. Am Mineral 88:713–724
Rodríguez Navarro C, Dohene E (1999) Salt weathering: influence of evaporation rate, supersaturation and crystallization pattern. Earth Surf Process Landf 24:191–209
Rodríguez Navarro C, Dohene E, Sebastián E (2000) How does sodium sulfate crystallize? Implications for the decay and testing of building materials. Cem Concr Res 30:1527–1534
Rodríguez Navarro C, Linares Fernández L, Dohene E, Sebastián E (2002) Effects of ferrocyanide ions on NaCl crystallization in porous stone. J Cryst Growth 243:503–516
Ruiz Agudo (2007) Prevención del daño debido a la cristalización de sales en el patrimonio histórico construido mediante el uso de inhibidores de la cristalización. PhD, University of Granada, Spain
Scherer GW (1999) Crystallization in pores. Cem Concr Res 29:1347–1358
Schiavon N, Chiavari G, Schiavon G, Fabbri D (1995) Nature and decay effects of urban soiling on granitic building stones. Sci Total Environ 167:87–101
Steiger M (2005a) Crystal growth in porous materials. I: The crystallization pressure of large crystals. J Cryst Growth 282:455–469
Steiger M (2005b) Crystal growth in porous materials. II: influence of crystal size on the crystallization pressure. J Cryst Growth 282:470–481
UNE 80-301-87 (1987) Cementos. Definiciones, clasificación y especificaciones. Primer complemento. AENOR, Madrid (Spain)
UNI-EN-1925 (2000) Metodi di prova per pietre naturali. Determinazione del coefficiente di assorbimento d'acqua per capillarità. CNR-ICR, Roma (Italy)
UNI-EN-1936 (2007) Metodi di prova per pietre naturali. Determinazione della massa volumica reale e della massa volumica apparente, e della porosità totale e aperta. CNR-ICR, Roma (Italy)
UNI-EN-13755 (2002) Metodi di prova per pietre naturali. Determinazione dell'assorbimento d'acqua a pressione atmosferica. CNR-ICR, Roma (Italy)
Van TT, Beck K, Al-Mukhtar M (2007) Accelerated weathering tests on two highly porous limestones. Environ Geol 52:283–292
Van Hess RPJ, Brocken HJP (2004) Damage development to treated brick masonry in a long-term salt crystallisation test. Constr Build Mater 18:331–338
Veniale F, Setti M, Rodríguez Navarro C, Lodola S, Palestra W, Busetto A (2003) Thaumasite as decay product of cement mortar

in brick masonry of a church near Venice. Cem Concr Compos 25:1123–1129
Watt D, Colston B (2000) Investigating the effects of humidity and salt crystallisation on medieval masonry. Build Environ 35:737–749
Winkler EM (1987) Weathering and weathering rates of natural stone. Environ Geol Water Sci 9:85–92
Winkler EM, Singer PC (1972) Crystallization pressure of salts in stone and concrete. Geol Soc Am Bull 83:3509–3514